Available online at www.CivileJournal.org

Civil Engineering Journal

(E-ISSN: 2476-3055; ISSN: 2676-6957)

Vol. 10, No. 09, September, 2024

Modeling of the Full-Scale Secondary Sedimentation Basin Using the GPS-X Model

Safi A. Hasan [1*], Basim K. Nile [1], Ahmed M. Faris [2]

[1] Department of Civil Engineering, Faculty of Engineering, University of Kerbala, Kerbala 56001, Iraq.

[2] Kerbala Sewerage Directorate, Kerbala 56001, Iraq.

Received 12 May 2024; Revised 13 August 2024; Accepted 20 August 2024; Published 01 September 2024

Abstract

The secondary sedimentation basin is being modeled in this study for the first time using the GPS-X model instead of the computational fluid dynamics (CFD) model. This study was conducted in the extended-aeration Al-Hur treatment plant that struggles with unstable sedimentation in its sedimentation tank. After collecting and entering the data into the GPS-X model, the model was calibrated and validated, and the results were statistically examined based on R and RMSE. To determine the efficiency of the sedimentation tank, the following scenarios were investigated: 1) testing the efficiency in removing pollutants; 2) conducting state point analysis (SPA); and 3) measuring the concentration of sludge in the layers of the sedimentation basin. Six factors were considered during the sensitivity analysis, namely sludge volume index (SIV), surface area, underflow rate (RAS), pumped flow (WAS), maximum settling velocity, and liquid temperature. The calibration and validation results were within the specified limits, and the secondary sedimentation basin demonstrated high efficiency in removing pollutants, with the analysis point (SPA) obtaining the highest MLSS concentration of 3000 mg/L. The sludge concentrations in the lower layers were 7000 mg/L, while those in the upper layer were 18 mg/L. These results suggest that a lower (100 ml/g) sludge volume index corresponds to a better sedimentation basin efficiency. Increasing the surface area of sedimentation basins can positively affect their efficiency, while increasing waste-activated sludge, maximum settling velocity, and liquid temperature may reduce pollutants and improve the sedimentation process. The GPS-X model is demonstrated as an excellent tool for understanding and predicting the work behavior of sedimentation basins, making this model particularly valuable for the management of sewage treatment plants.

Keywords: Sedimentation; GPS-X; SVI; Maximum Settling Velocity; State Point Analysis.

1. Introduction

Secondary settling basins (SSBs) play crucial roles in the production of clarified effluents. Secondary settling is the ultimate stage of biological sewage treatment processes that use activated sludge (AS). Another important role of SSBs is effectively increasing the viscosity to obtain a highly concentrated mixture of recycled sludge and biomass inside biological reactors. The optimal functioning of these reactors typically requires the removal of biomass from sewage via sedimentation, filtering, or other methods of separating solids from fluids. While various treatment processes can efficiently separate solids from liquids but secondary settling basins (SSBs) are most frequently employed for these purposes [1]. These basins, which are also referred to as sedimentation tanks or solid-fluid separators, use gravitation to isolate the biomass from the liquids, thus serving two unique yet comparable purposes: clarifying and thickening [2, 3]. Clarifying involves eliminating small solid particles from a fluid to produce clear and less turbid effluents, while

* Corresponding author: safi.abed@s.uokerbala.edu.iq

http://dx.doi.org/10.28991/CEJ-2024-010-09-017

thickening involves increasing the sludge concentration to enable its reuse or disposal in smaller volumes. The clarification operation takes place in the upper region of SSBs, while thickening predominantly takes place in the lower region of these basins [4].

The upper region of SSBs discharges effluent waste, which includes a smaller number of solid particles, while their lower region receives a separate flow of settled, highly concentrated biomass suitable for reuse or disposal. While SSBs play critical roles in sewage treatment operations, they may also restrict the whole operation [4, 5]. The sizing of SSBs must be integrated with that of the bioreactor to meet the minimum required conditions, such as solids retention time (SRT) or food-to-microorganism ratio (F/M), in designing specifications. Additionally, a safety factor should be maintained to manage unexpected disturbances and upsets. If SSBs fail to generate a clarified effluent or are unable to increase the concentration of microorganisms to the desired level for recycling, then excessive solid waste will be generated, thus violating the effluent specifications and resulting in reactor microorganism loss. Studies on the design of secondary tanks for treatment operations have relied on the surface overflow rate of the tank and assumed that this flow is uniform and unidirectional. However, some studies point to a non-ideal flow behavior in sedimentation tanks that can be explained by several factors, such as inlet and outlet geometry and flow disorders. These tanks also experience dead zones, solids resuspension, and temperature variations.

Liquid waste undergoes multiple stages of treatment, including biological and physical processes, pathogen sterilization after treatment, thickening, drying, or incineration for excess sludge. The treatment process in secondary tanks focuses on influent filtration. Carefully designing SSBs and enhancing their biological operation to enhance sedimentation efficiency can help achieve influent filtration at a lower cost. Understanding those factors that influence sedimentation efficiency in the AS process is also crucial. In most cases, the concentration of total suspended solids (TSS) determines the oxygen demand (BOD) in influent treatment, and the BOD value can be lowered by reducing the influent (TSS). Storing AS is also a necessary precautionary measure during periods of high flow rates [1, 5]. The conditions within the biological reactor can impact the sedimentation and clarifying properties of the sludge. For instance, under-aeration decreases the sludge settling capacity, while over-aeration can produce small flocs that may result in inadequate clearing in sedimentation tanks.

Although sludge usually has excellent settling properties, there are times when these properties are not excellent enough, particularly in operations where a significant percentage of the sludge is purposely unaerated, such as when eliminating nutrients. Therefore, the biological process and the SSB have interdependent functions, making it impossible to design one without the other. If any of these two operation units fail, then the design goals cannot be achieved [6]. The SVI is an operational control parameter that quantifies sludge settling behavior in the aeration basin of an AS operation. Since its introduction by Mohlman (1934), SVI has become a widely accepted standard for assessing the physical characteristics of AS operations. For example, researchers often use SVI to determine if the expansion of troublesome filamentous organisms, which leads to inadequate settling in secondary clarification procedures, is the cause of operational problems [7]. The term “activated SVI” refers to the measured volume (in ml) occupied by 1 g of AS after allowing the aerated liquid to settle for 30 minutes.

Introduced by Donaldson, the sludge density index is computed as the reciprocal of SVI multiplied by 100. Both of these indexes were designed to serve as approximate indicators of sludge settleability and were intended to be utilized in the daily operation of sewage treatment plants, specifically for monitoring the physical state of AS. The simplicity in testing SVI has led to the widespread use of this metric in applications beyond its original purpose. The SVI is also among those parameters that are used to determine the necessary sludge recycling rate and the concentration of suspended particles in mixed liquor suspended solids (MLSS) [7, 8].

Since the beginning of the 19th century, scientists have recognized the effect of temperature on the rate of sedimentation and the sedimentation process in general. Hazen (1904) proposed that suspended particles settle quicker when the liquid is warmer and added that the settling basin works twice as hard in summer as in winter [6]. Many studies have also indicated that temperature differences affect the performance of sedimentation tanks. In other previous studies, it was proposed that cold water sinks and replaces warmer water and that the tank removal efficiency varies across seasons, especially during summer and winter when temperatures are at their highest. Kriš & Hadi (2008) observed that the excess suspended materials increase along with decreasing temperature [9].

Raeesh et al. (2023) studied the turbulence in the sedimentation tank of water and wastewater plants by using computational fluid dynamics (CFD) [10]. Lasaki (2023) et al. utilized mathematical programs to study the pollutant removal performance of primary sedimentation tanks of wastewater treatment plants [11]. Dairi et al. (2023) used CFD to improve the performance of secondary sedimentation tanks [12]. Wu et al. (2024) conducted numerical simulations (Mixture and RNG k-ε) to determine those operating factors that influence the performance of sedimentation tanks [13]. Poorkarimi et al. (2024) used CFD to investigate the efficiency of sedimentation basins [14].

However, sedimentation tanks suffer from instability in terms of settling materials and working efficiency under different organic loads.

Model simulation is a valuable tool for optimizing complex biological handling processes and for redesigning and administering sewage treatment plant systems. One of the most used simulation software in the commercial sector is the GPS-X Model version 8.0 developed by Hydromantis Inc. in Canada. The GPS-X simulator incorporates the AS simulations evolved by the International Water Association, namely, ASM1, ASM2D, and ASM3, and the models developed by Hydromantis, specifically Mantis1, Mantis2, and Mantis3 [15]. Similar to any other biological model, the accuracy of the data generated from GPS-X is contingent upon the model calibration. These software packages have been developed to cater to the needs in engineering practice [16].

The GPS-X model demonstrates advantages in facilitating and streamlining the construction of models, conducting simulations, and interpreting findings. These advantages can be attributed to its utilization of a sophisticated graphical user interface. Consequently, this model has been extensively employed to simulate sewage treatment plants and enhance their operational efficiency [17]. The necessity of model calibration arises when there is a lack of agreement between the outcomes of a simulator and the experimental laboratory findings. To calibrate the GPS-X model, it is necessary to acquire past information about the influent and effluent sewage variables. The GPS-X model also allows for the adjustment of kinetic and stoichiometric variables within a certain range to align the simulation outcomes with the experimental findings [18]. Accordingly, some researchers have utilized this model to simulate a batch reactor operation across several scenarios in various sewage treatment plants.

Considering the aforementioned advantages, this study uses the GPS-X model to measure the efficiency of SSBs and determine the most important factors that affect their efficiency. This study was conducted in three scenarios. The first scenario assessed the pollutant removal ability of SSBs, the second scenario conducted a state point analysis (SPA), and the third scenario examined the amount of sludge present in the layers of SSBs. The sensitivity of these SSBs was determined by five factors, namely, surface area, SVI, maximum settling velocity (SV), pumped flow (waste AS or WAS), and underflow rate (return AS or RAS).

This study utilized the GPX-S model because of its rapid procedures for simulating and analyzing the sensitivity of all elements affecting wastewater. The GPX-S model assists the operating engineers in the design and operation of the stations, managing the load shock fluctuations to which the station is susceptible, and enabling them to control all pollutants. By adjusting specific parameters within the operating panels of all station parts, from the liquid waste entry point to all stages of the treatment parts, whether physical or biological, the GPX-S model assists the operating engineers in controlling all pollutants. The CFD focuses on a specific part of the station. It is also possible to use the GPX-S model. Improving the operation of the station and adding other parts within the station units increases the efficiency of the station and reduces maintenance and operation costs.

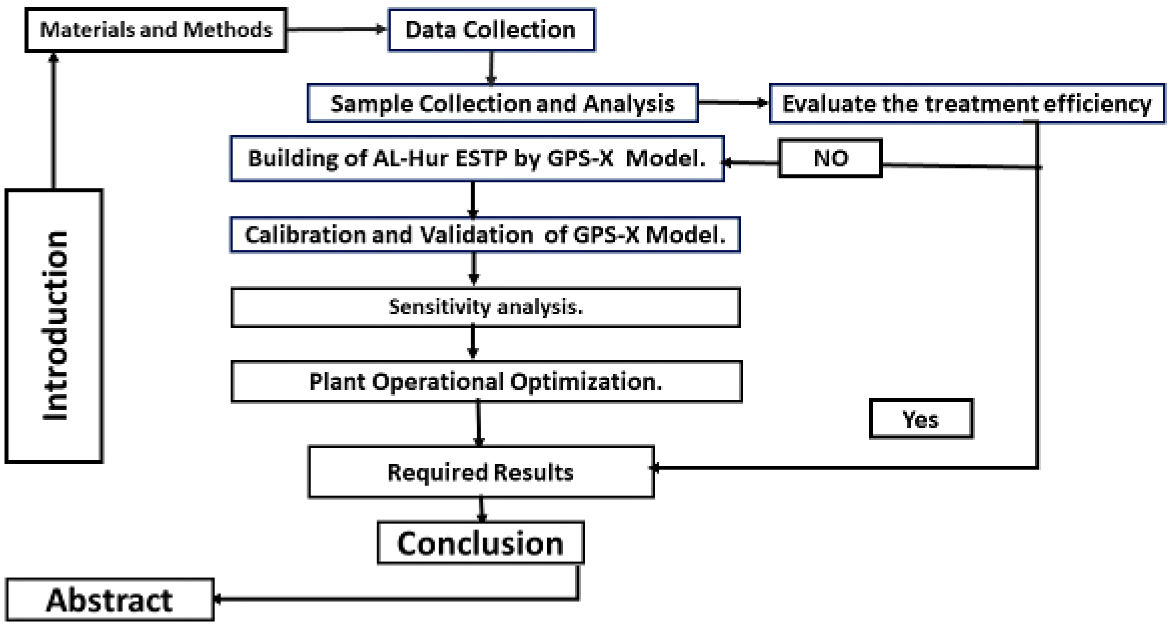

Figure 1. Structure of article

2. Material and Methods

2.1. Research Framework

A research methodology elucidates the comprehensive approach used in a study to achieve its objectives. Figure 2 presents the adopted research framework.

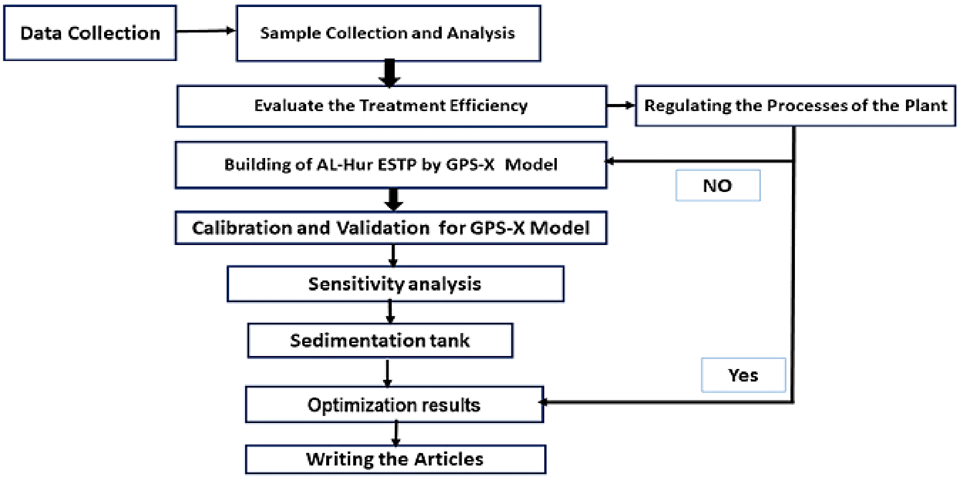

Figure 2. Study framework

2.2. Site Location and Description

Case Study

The Al-Hur sewage treatment plant (A-STP) is located south of the Iraqi capital, Baghdad, and within the administrative borders of the Karbala Governorate with geographical coordinates of 32.6899016°N and 43.9806550E (Figure 3). The A-STP was designed with a daily discharge rate of 37,000 m^3/d, and the treatment plant operates within this rate and sometimes exceeds the design capacity. The plant operates with an AS system during extended aeration processes. The biological nutrient removal system is of type A2/O (anaerobic, anoxic, and oxic). The A-STP involves four levels of treatment, as shown in Figure 4. The first level is the preliminary treatment, which involves the use of coarse and fine screens and a grit and oil removal chamber. The second level focuses on biological treatment to remove organic materials and nutrients and involves the use of anaerobic, anoxic, aeration, and sedimentation tanks. The third level involves the disinfection process, where chlorination is applied to remove pathogens. The fourth level involves sludge treatment and stabilization.

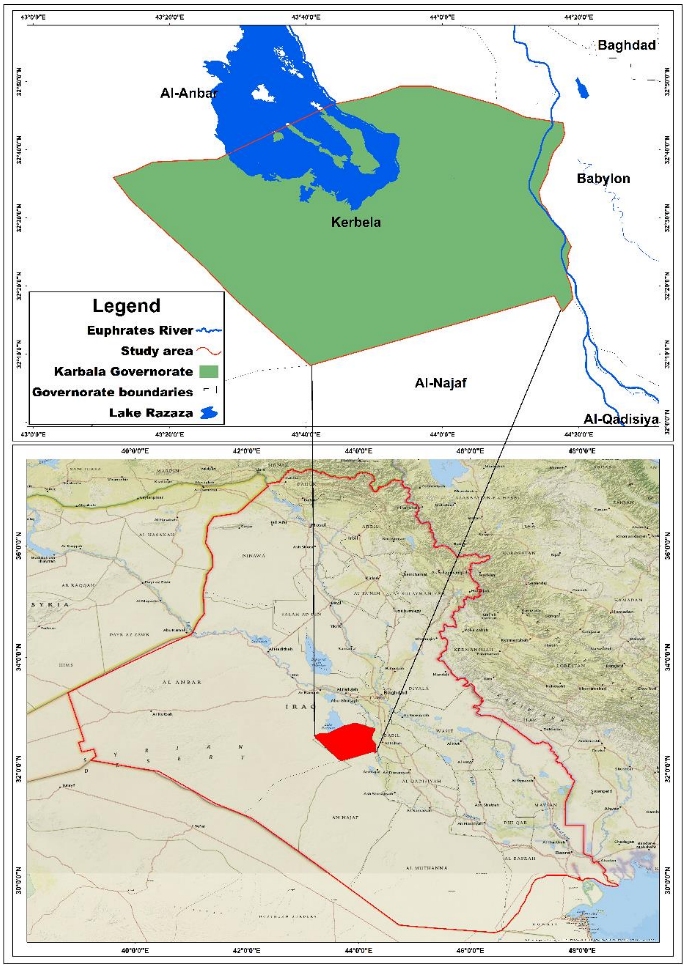

Figure 3. Al-Hur sewage treatment plant (A-STP)

Figure 4. Al-Hur sewage treatment plant (A-STP)

Efficiency of the Secondary Sedimentation Basin

Extended aeration processes are distinguished from conventional AS systems by the absence of primary sedimentation basins [19]. The A-STP contains four secondary sedimentation basins that operate in accordance with the statements shown in Table 1. The efficiency of these SSBs was evaluated based on three key factors, namely, the pollutant effluent, state point analysis, and TSS concentration in the depth layers of the SSBs. SPA, which is considered one of the most important parameters for determining the operating efficiency of SSBs, offers a straightforward mathematical model for assessing the performance of SSBs based on six factors. However, the graphical output of SPA needs to be carefully interpreted. SPA is also a useful method for illustrating the operational state of sedimentation. This analysis is founded on a graphical representation of the solid's mass balances around the sedimentation. The procedure incorporates inherent simplifications, including the following:

- Steady-state circumstances as its foundation;
- Considering only one (perpendicular) dimension and ignoring short circuiting or the characteristics of the sludge disposal process;
- Ignoring compression; and
- Ignoring TSS in the effluents.

Despite these simplifications, SPA is often utilized in the predesign stage to determine the clarifier surface and the return pump ability and in the process stage to predict the maximum MLSS and the necessary return flow settings prior to fine-tuning the station's actuation while taking into account its actual performance. The secondary sedimentations are evaluated based on two primary sets that encompass hydraulic loading rate (HLR) and solid loading rate (SLR).

Any of these design characteristics can limit the overall performance of the clarifier, even though the SLR is the most crucial factor in deciding whether secondary clarifiers will function. State point examination is a simplified mathematical simulation that uses real operational data to predict the secondary clarification efficiency, including influent flow rate, RAS flow rate, MLSS concentration, sedimentation tank surface area, number of sedimentation tanks in valeting, and SVI. The intersection of the surface overflow rate line and the solids in the sedimentation WAS rate line are referred to as SPA. The state point needs to be situated well under the settling flux involute for the secondary clarifiers to operate steadily, where the sludge blanket is kept at $\leq$ 3 ft. The sludge blanket in the sedimentation tank is expected to become thicker as the state point approaches the limit line as indicated by the flux involute. The solid underflow line approaching or becoming tangent to the settling flux curve provides further proof. The solids of the clarifier will be lost when the state point has jumped external or exceeds the settling flux curvature.

2.3. Sampling and Analysis

Laboratory specimens were gathered from 1/2/2023 to 1/2/2024 to evaluate the effectiveness and performance of the A-STP as shown in Table 2. The data was collected from the wastewater influent the plant and the effluent waste leaving the plant from the Karbala Sewage Directorate from Al-Hur A-STP, plant for a year, at a rate of 10 samples per month over the different seasons of the year. Analyzed the data collected in the Al-Hur plant laboratory and evaluated it with established standard methods for assaying water and wastewater [20]. The findings were then compared with the Iraqi standards for sewage [21, 22]. The process encountered challenges due to fluctuations in loads and temperatures in the study area, as well as the environmental risks posed by the station due to pollutants and gases from biological treatment processes, including the release of nitrogen gas, hydrogen sulfide, and other pathogens.

Table 1. Properties of the sedimentation tank

Parameter	Value
Flowrate (m^3/d)	37000
Surface area for secondary final clarifier (m^2)	3200
Sedimentation tank type	circular
Sedimentation tank diameter (m)	32
No. of Sedimentation tanks	4
Depth of side wall (m)	3.5
Centre wall depth (m)	6.5
Mixed liquor suspended solids (MLSS) (mg/L)	1250-3500
Hydraulic Loading Rate (HLR) (m^3/m^2d)	11.5
Returned Activated Sludge (RAS) %	75
Solids Loading Rate (SLR) ($kg/m^2.h$)	1.25
Waste Activated Sludge (WAS) (m^3/d)	952
Food to Microorganism (F/M)	0.04
Hydraulic Retention Time (HRT) (h)	> 3
Sludge removal mechanism	scraper
Sludge volume index SVI (ml/g)	80
Average Inflow temperature (°C)	12 in winter and 37 in summer

Table 2. Properties of inlet and outlet sewage for A-STP

Parameter	Inlet, mg/L	Outlet, mg/L	Standard IRQ Regulation No. 25 of 1967 protects rivers and public water from pollution [22]
COD	350	23	< 100
BOD_5	140	10	< 40
TSS	160	18	60
PH	7.18	7	6-9.5
Nitrate (NO_3)	ND	55	50
Nitrite (NO_2)	0.4	0.2	Nil
Ammonia (NH_3)	31.6	0.3	10
PO_4-P	6	3.2	3
H_2S	31	ND	3
Oil & grease	53	3	4

*= unit less

2.4. Sedimentation Model

This study used the GPS-X simulation program version 8 (educational license), which is used in designing and simulating the operations of processing plants with high quality. GPS-X also helps enhance the design quality and operational efficiency when designing a new plant or simulating an existing plant [16]. The primary phases involved in generating a GPS-X model include model building, model calibration, scenario preparation, simulation, and outcome analysis. The most critical stage in this operation is model calibration, given that a simulation model must encompass all physical operations of the actual plant and demonstrate a comparable performance to assess its functionality appropriately. Unlike previous studies that rely on CFD, the SSBs in this study were simulated using a GPS-X model. GPS-X categorizes the sedimentation simulations as nil-dimensional (point), one-dimensional (1d suffix), interactive (mantis, asm1, ...), or unreactive (simple):

- Nil-dimensional, unreactive: point.
- Simple1d: a 1D system that is unreactive.
- The system is interactive and one-dimensional, featuring features like mantis, asm1, asm2d, and asm3, along with new general features.

Interactive models incorporate biological reactions and are named after the equivalent suspended-growth models. As an illustration, the mantis sedimentation simulations employ the mantis suspended-growing concept. As seen in Figure 5, one-dimensional simulations partition the settler into a specified number of stratums (often 10) of uniform thickness.

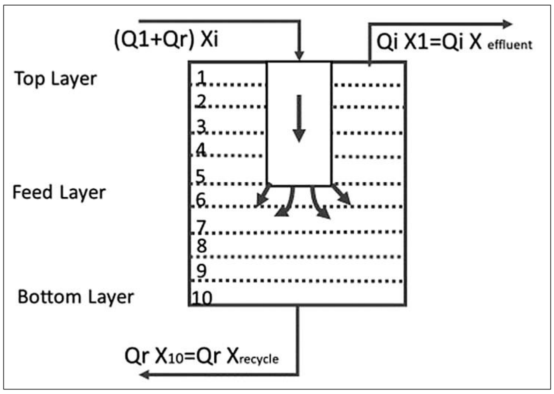

Figure 5. 1D sedimentation model

The simulations were conducted following the solid flux concept. A mass balance was applied for each stratum to simulate the distribution of solids all the way through the settled column beneath each of the steady-state and dynamic conditions. As shown in Table 3, the befitting involvement of each stratum of the settler to the mass balance. It is noticed the presence of five different groups of stratums based on their location correlated to the feed point, as seen in Figure 6. These simulations also depended on the conventional solids flow examination. However, the solid flux inside a specific stratum is constrained via the capacity of the neighboring layer for handling this solid. The solid flux resulting from the movement of the fluid bulk can be easily determined by increasing the solid concentration via fluid bulk velocity, which can be either upward or downward reliance on the correlation of its location to the feed stratum.

The sedimentation-induced solid flux is determined through a dual exponential settling function, which is applied to impeded sedimentation and flocculant sedimentation circumstances. Equation 1 presents the settling operation as outlined by Takács et al. [23].

Table 3. Sedimentation paragon: input-output summary

Layer	Input			Output	
	Feed	Settling	Bulk liquid Flux	Settling	Bulk liquid Flux
Top	-	-	UP	+	UP
Layer above the feed point	-	+	UP	+	UP
Feed	+	+	-	+	Up-down
Layer above the feed point		+	down	+	down
Bottom		+	down	-	down

Note: + = Phenomenon considered, - = Phenomenon considered.

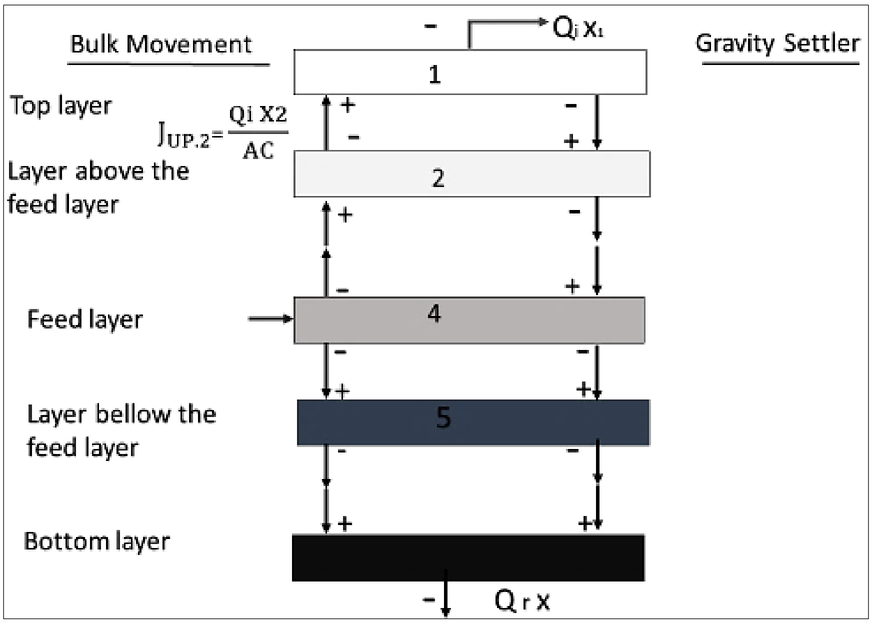

Figure 6. Solids balance around the settler stratums

$$v_{sj} = v_{max}\, e^{-rhin.\, X_J^O} - v_{max}\, e^{-rfloc.X_J^O} \tag{1}$$

where: v_{sj} = SV in layer j (m/d); v_{max} = maximum Vesilind SV (m/d); $rfloc$ = flocculants region settling parameter (m^3/g TSS); and: $X_J^O = X_i - X_{min}$. Where X_{min} is the minimum of suspended solids concentration that can be accessible, and X_J is the concentration of suspended solids in stratum J.

Equation 2 calculates the minimum accessible solids focus in a stratum, X_{min}, as a fractional (unsettleable part, or fns) of the impact solids focus to the settler.

$$X_{min} = fns \times X_{in} \tag{2}$$

The value is limited by the employed to a maximum value known as the maximum unsettleable solids, or Xminmax. The SV decreases and reaches its minimum value of zero. If the user enters parameter values that result in a negative SV, then a caveat missive will be shown in the simulation log box. The SV is limited by an employed-defined maximum value known as the maximum SV or $Vbnd$. Figure 7 displays the settling function and highlights four distinct zones. First, the SV becomes zero when the solids reach the lowest possible concentration. Second, the flocculating properties of the particles primarily influence SV. Therefore, SV is highly responsive to changes in the $rfloc$ parameter. Third, the SV reaches a point where it is no longer affected by the concentration of solids, indicating that the particles have achieved their maximum size. Fourth, the SV is influenced by hindrance and becomes contingent on the parameter (the simulation simplifies to the Vesilind equation).

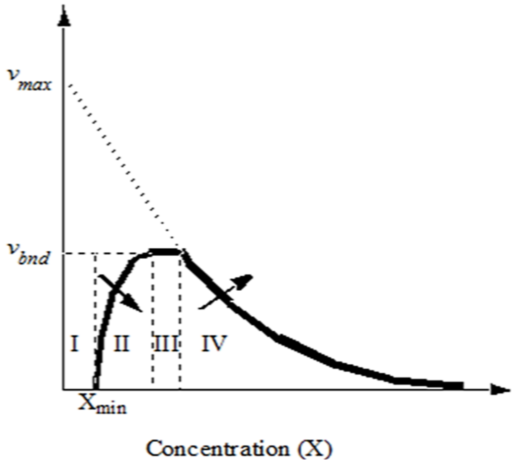

Figure 7. Settling velocity vs. concentration

SS concentration is the sole variable that is numerically integrated into the simple 1D sedimentation model. This model can only be applied if the biological reactions of the settler can be disregarded. This settler is influenced by many particle state variables, such as heterotrophic organisms, which are stocked as part of the TSS concentration. After each numerical integration stage, the model restores the concentrations of particle state changeable in the effluent, underflow (RAS), and pumped flow (WAS) by utilizing the breakages obtained from the numerical incorporation of the SS in the settler stratums [24]. The concentrations of dissolve state variables remain unchanged in the simple1D model. The dissolved state variables in the unreactive by models experience complete mixings throughout the region, unlike the particulate ingredients, which migrate across different layers. The sedimentation simulations of the GPS-X model for secondary sedimentation tanks consider the correlation among the settling parameters and SVI data. The SVI test distinguishes the depositon that happens in the sedimentation tank's high solids focus band an additional parameter, known as the clarifying factor, is required to precisely define the sedimentation properties across the whole range of concentrations and the settling behavior in areas with flocculant or a few solid concentrations. This element measures the degree of clarification, with a value of 1.0 indicating a high level of clarification and a value of 0.1 indicating a low level. The correlation equations are as follows:

$$\boldsymbol{v_{max}} = \text{fcorr1} + (\text{fcorr2 . SVI}) + (\text{fcorr3. SVI}^2) \tag{3}$$

$$rhin = \text{fcorr4} + (\text{fcorr5 . SVI}) + (\text{fcorr6. SVI}^2) \tag{5}$$

$$rfloc = \text{fcorr7} + (\text{fcorr8 . SVI}) + (\text{fcorr9. SVI}^2) \tag{6}$$

where, v_{max} = maximum Veslind SV(m/d); $rhin$ = Hindered Region Settling Parameter (m^3/g TSS); $rfloc$ = flocculant region settling parameter (m^3/g TSS).

SVI = SVI (mL/g).

clarify = clarification factor.

$fcorr1 - fcorr9 = SVI\ relationship\ modules.$

In order to utilize the correlation, the employed is required to enable the utilization of the SVI parameter for estimating settling parameters by setting it to ON. GPS-X automatically calculates the settling parameters after determining the SIV and sedimentation tank parameters. The correlation modulus can be obtained by navigating to the choices > General statements > System > Parameters > Miscellaneous form.

2.5. GPS-X Model Calibration and Validation (AESTP)

Calibration involves changing a model's default parameters such that its predictions correspond to datasets from a real WWTP. In other words, this process aims to reduce the discrepancy between the model's predictions and the actual treated wastewater pollution concentrations. We conducted this investigation's calibration over the spring and summer, spanning a total of six months. Model validation refers to the agreement—within reasonable bounds—between the model's predictions and different sets of statements that are not used in the construction of this model. In this study, the validation was conducted over autumn and winter, also spanning six months [25]. Figure 8 shows that model calibration and validation processes achieved a steady state. Table 1 indicates that during the calibration phase, we selected groups of sensitive factors related to the operating conditions, wastewater characteristics, volumes, and dimensions. These same factors were also used in the validation process. Spanning several periods in the fall and winter [26], following, the prediction results were statistically examined using root mean square error (RMSE) and correlation factor (R) to validate the calibration.

$$R = \frac{\overline{(C_O - \overline{C_O})(C_P - \overline{C_P})}}{\sigma_{C_O}\sigma_{C_P}} \tag{7}$$

$$RMSE = \frac{\overline{(C_O - C_P)^2}}{\overline{C_O}\ \overline{C_P}} \tag{8}$$

Where C_O (mg/L) explains the actual statements; C_P (mg/L) explains the modeled statements; $\overline{C_O}$ is the rate of the actual statements; $\overline{C_P}$ is the rate of the modeled statements; and (σ) is the standard deviation from the collection's statements. The statistical norms for tolerable limitations are defined as $1 \geq R > 0.8$ and $0 \leq RMSE < 1.5$. Figure 8 illustrates the graphical procedures for the model calibration and validation employed by Zwain et al. [27].

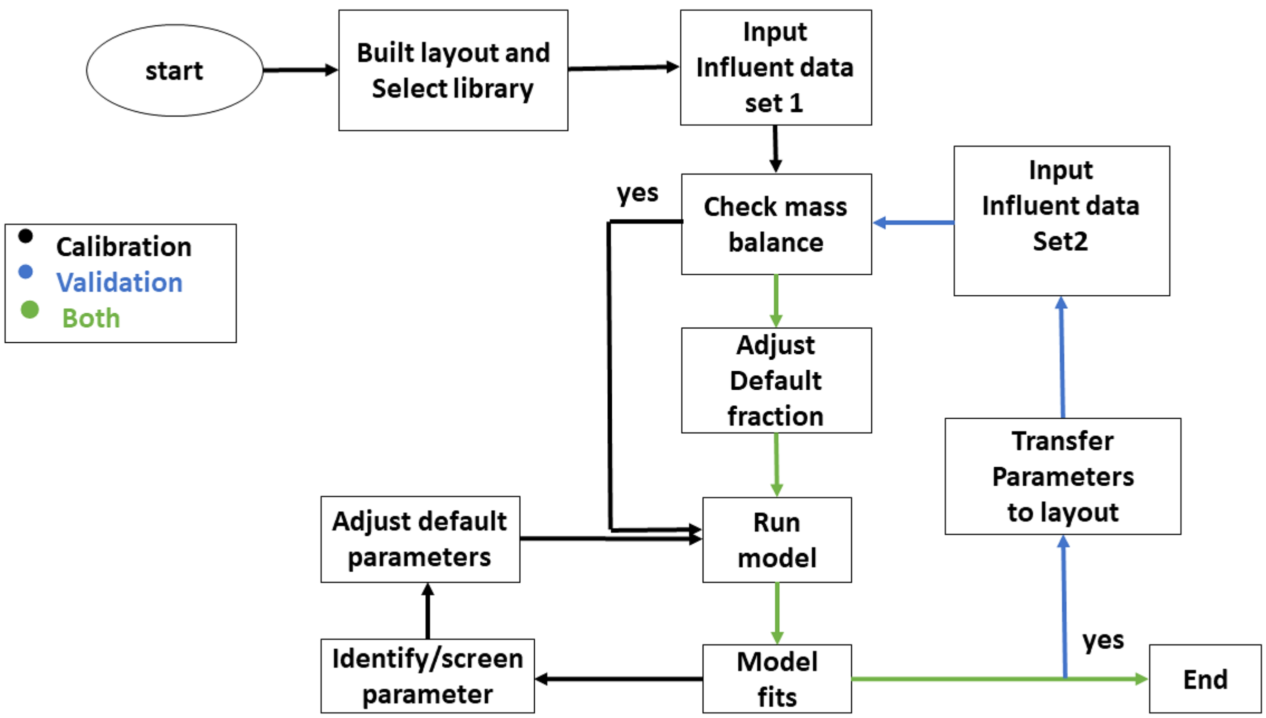

Figure 8. Procedure for the model calibration and validation

2.6. Sensitivity Analysis

Sensitivity analysis aims to define the sensibility of the simulation model's output variables (follower variables) to the modifications in its parameters (independent variables). The sensibility analysis results are particularly useful when setting up a parameter assaying run given that these results help identify those parameters that must be modified by the improver. Any model requires a sensitivity analysis for two key reasons:

- To calibrate the model findings, and
- To determine parameters to be modified through validation.

Model calibration should grant the modeler enough confidence in its ability to perform as expected. Parameter determination is useful in sensitivity analysis as it helps identify those parameters that greatly impact the model response. In this study, the parameters were not modified during the calibration process due to their minimal influence on the typical behavior of the model. After calibrating and validating the model, a sensitivity analysis can be performed to investigate other issues. Mathematical models may also be used as reagents to investigate operational strategies that might not have been considered otherwise. Accordingly, a sensitivity analysis for a full-scale SSB at the A-STP was performed in this study. Six sensitive factors on which this SSB strongly depends were selected, and their impact on the station's efficiency was examined. These factors include SVI (50 ml/g–350 ml/g), surface area (804 m^2–3216 m^2), RAS) (7000 m^3/d–56000 m^3/d), WAS) (250 m^3/d–4500 m^3/d), maximum SV (50 m/d–500 m/d), and liquid temperature (18°C–37 °C). The layout of the Hur A-STP in the GPS-X model is shown in Figure 9.

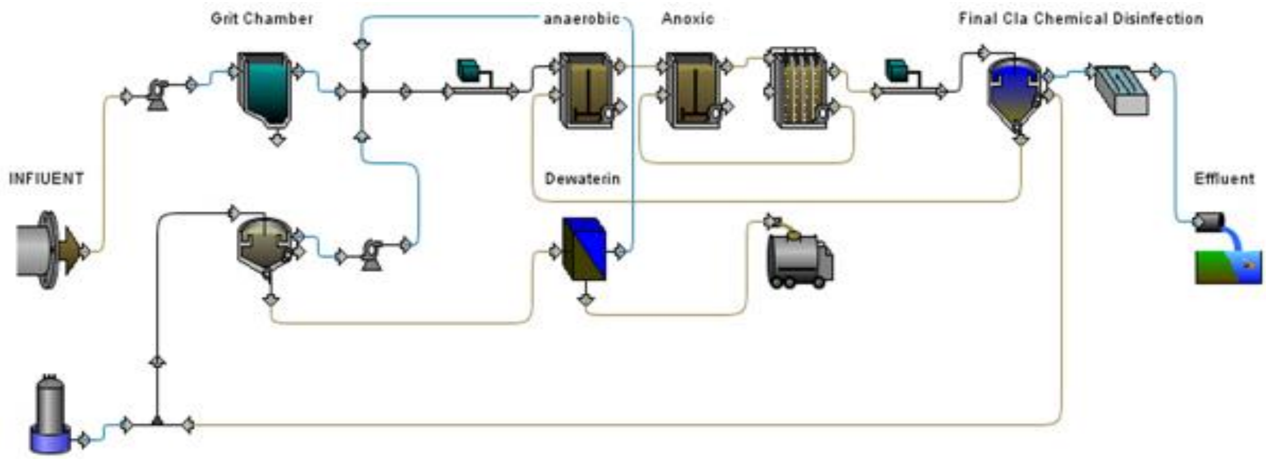

Figure 9. Layout of the Hur A-STP in the GPS-X model

3. Results and Discussion

3.1. Performance of the A-STP Sedimentation Basin

The SSB of A-STP was evaluated in consideration of three basic factors. The first of these factors is the effluent of pollutants after sedimentation, especially TSS. The TSS elimination efficiency in the final sedimentation tank was greater than 95%. The second factor is SPA, which determines the efficiency of the final sedimentation tank. Figure 10 displays the state-point analysis of the A-STP's secondary sedimentation basin. According to the results shown in Figure 10, the sedimentation tank's performance efficiency is excellent because the red dot is located inside the solids' settling flux curve. In addition, the cross of overflow flux and underflow (RAS) flux resulted in the best MLSS concentration of 3000 mg/L. The analysis point provides an excellent impression of the RAS and WAS processes, which intersect at the middle of the settling flux curve.

The analysis point also shows that any change in RAS or WAS would decrease or increase the concentration of MLSS and thus reflect negatively on the performance of the sedimentation process. As long as the operation point (red dot) stays within the red curve and the green line does not cross this point, the operating condition of the clarifier is considered safe. The third factor is the sludge concentration in the SSB layers. Extended aeration processes have the advantage of producing less sludge than conventional activated sludge systems. Figure 11 shows the concentrations of TSS for each SSB layer. The first seven layers demonstrate an excellent efficiency and do not exceed the threshold limits stipulated in the Iraqi specifications as mentioned in Table 2. Meanwhile, the sludge concentration increases at the bottom of the sedimentation basin, especially in the last layers, where the sludge concentrations exceed 6500 mg/L.

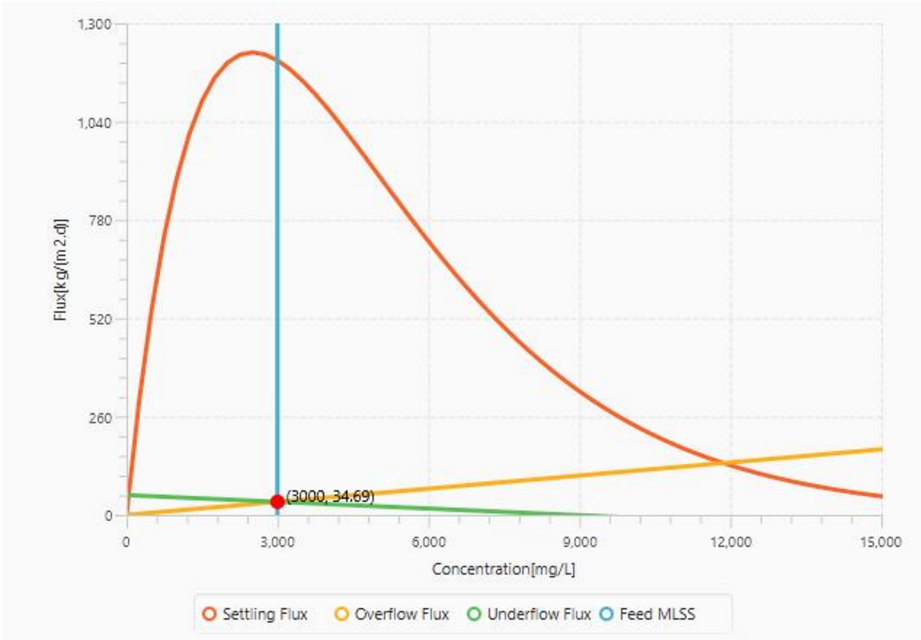

Figure 10. State point analysis (SPA) graph

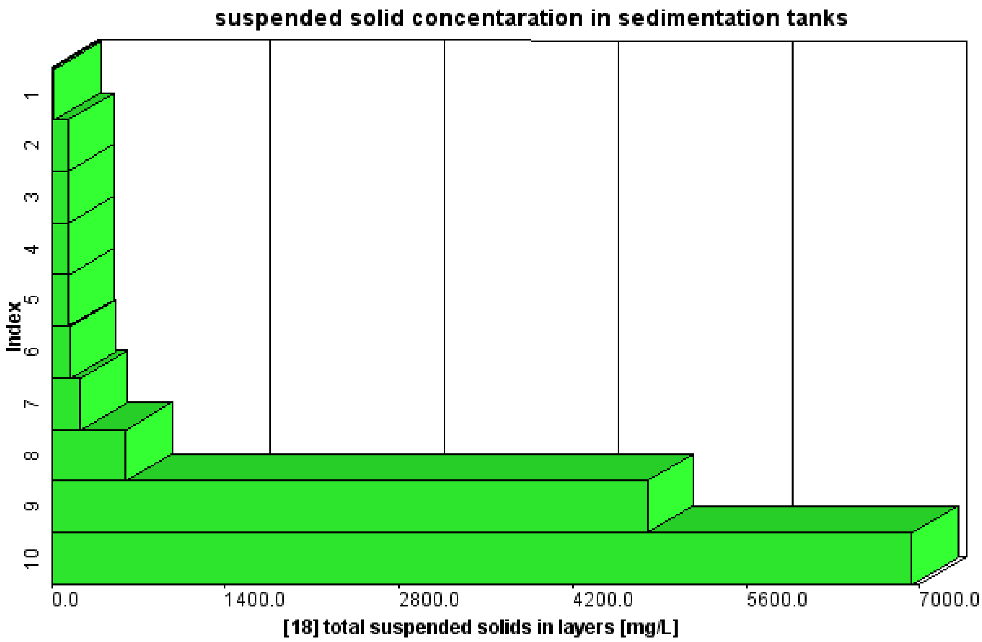

Figure 11. Clarifier profile graph

3.2. Model Calibration for A-STP

When utilizing simulation systems to expedite labor improvements and abbreviate time, it is imperative to conduct laboratory auditions, calibration, and validation in a manner that guarantees that the model's outputs closely resemble reality. The model in this study was calibrated by utilizing the average effluent wastewater from the A-STP during spring and summer. This model was then validated by utilizing measurements captured during autumn and winter. The model started to run using the default statements and produced findings that greatly differed from the real values [28]. Adjusting many essential parameters significantly impacted the results as presented in Tables 4 and 5. Some of the most sensitive parameters (stoichiometry and kinetic parameters) were then modified to bring the predicted plant effluent closer to the actual results. Figure 12 presents the results after applying the modifications shown in Tables 4 and 5. These results were statistically examined based on R and RMSE to make them more acceptable. The pollutants coming out of the station were also examined, and they all conformed to the limits for R and RMSE as shown in Table 6. After obtaining acceptable results, the model calibration was terminated. Several sensitive parameters were then chosen to achieve outputs that closely resemble reality.

Figure 12 demonstrates that the default TSS readings were below 5 mg/L, indicating a significant deviation from the actual values. As a result, the sensitive parameters in the GPS-X model related to the final sedimentation tank were adjusted. Specifically, the feeding point was moved from the bottom from the default value of 1 m to the actual value of 4.8 m, and the maximum Vesilind SV was increased from 410 m/d to 1330 m/d because these two parameters exhibited the greatest sensitivity among all other operational parameters. Furthermore, the levels of COD and BOD exceeded their actual values, thus prompting the adjustment of certain sensitive parameters as presented in Tables 4 and 5 to effectively reduce these concentrations. By contrast, the initial nitrate concentrations were significantly greater than the actual values, and this discrepancy was rectified by adjusting those sensitive parameters that are associated with the kinetics and stoichiometry parameters of ammonia and nitrates. Nitrogen fractions and active heterotrophic biomass were identified as crucial factors that accurately aligned the predicted nitrate level values with the actual values. Given that the default values of phosphates exceeded the actual values, the phosphorus fractions were modified to improve the alignment between the projected outcomes and the actual values.

Table 4. GPS-X enter stoichiometry parameters (default & adjustment) based on GPS-X influent advisor

Influent Stoichiometry Composition			GPS-X Default	Calibration	Verifications
Classification Parameter	**Parameter**	**Unit**		**Spring and Summer Averages**	**Autumn and winter averages**
Influent Fractions	*Ivt*	gVSS/gTSS	0.75	0.7	0.72
Organic Fractions	*Frsac*	-	0	0.015	0.015
	Frxbh	-	0	0	0
	Frxi	-	0.13	0.079	0.078
	Frsi	-	0.05	0.01	0.01
	FrsS	-	0.2	0.02	0.02
Nitrogen Fractions	*Frsnh*	-	0.9	0.9	0.9
	inSi	gN/gCOD	0.05	0.04	0.039
	inXi	gN/gCOD	0.05	0.01	0.01
Phosphorus Fractions	*ipSi*	gP/gCOD	0.01	0	0
	ipXi	gP/gCOD	0.01	0.011	0.012

Table 5. The stoichiometry and kinetic parameters of the A2/O GPS-X default and adjusted models are Similar for calibration and verifications results.

Influent Stoichiometry Composition			GPS-X Default	Calibration	Verifications
Classification Parameter	**Parameter**	**Unit**		**Spring and summer averages**	**Autumn and winter averages**
physical	*v*	m^3	1000	51000	51000
	d	m	4	5	5
Model Stoichiometry Parameters					
Active (aer.het.yi. solu. sabst.)	*YH*	gCOD/gCOD	0.666	0.574	0.574
Heterotrophic Biomas (unbiod.frac Cell decay)	*UH*	gCOD/gCOD	0.08	0.05	0.036
Active (yield ferment. biomass)	*YH*	gCOD/gCOD	0.18	0.35	0.35
Autotrophic Biomass (unbiod. frac. decay)	*UH*	gCOD/gCOD	0.08	0.01	0.036
Kinetic Parameters					
Active (max.spcif. growth rate.subst.)	*μ max.H*	1/d	3.2	3	3
Heterotrophic Biomass (aer.het. dacy rate)	*bh*	1/d	0.62	1.4	1.4
Active (max. growth. Rate ammon.Oxid.)	*μ max.H*	1/d	0.9	0.8	0.8
Heterotrophic Biomass (Ammon.sat.coeff. Ammon.Oxid)	*KNH*	mgN/L	0.7	0.6	0.61
Hydrolysis	*xs/kh*	1/d	3	3	3
	Khxs	-	0.1	0.1	0.1

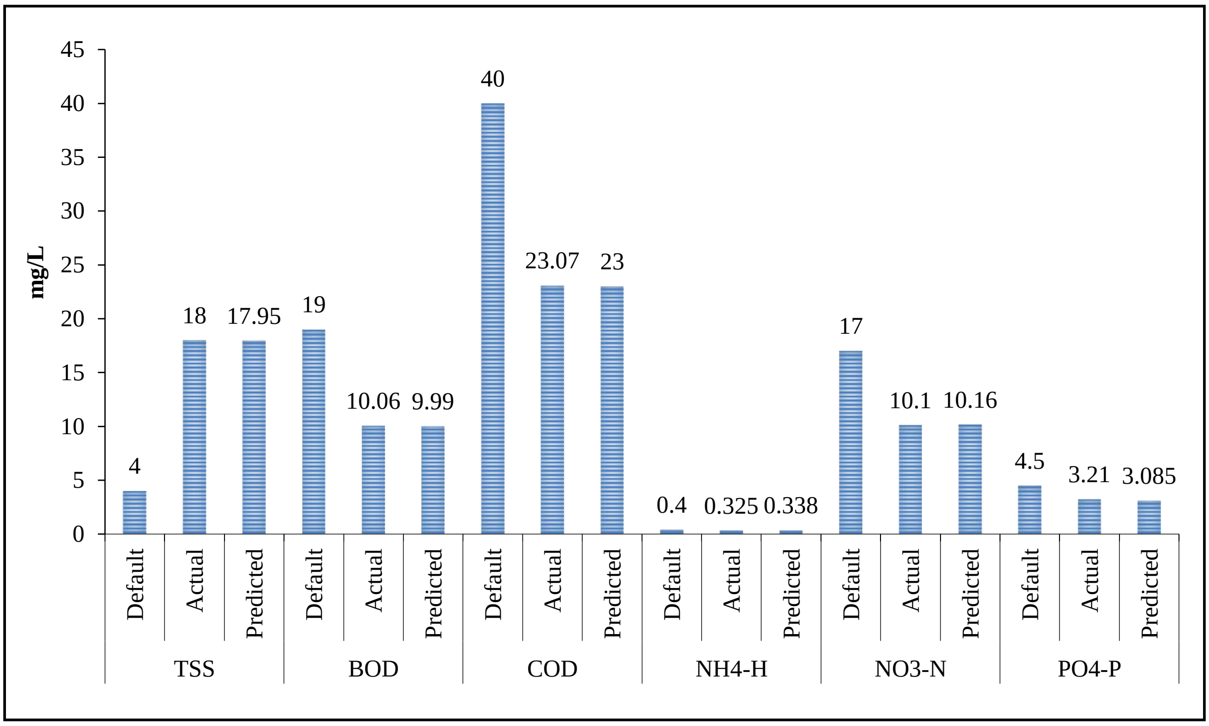

Figure 12. Calibration of the actual and predicted values

3.3. Model validation for A-STP

During the model validation, the alignment between the findings and the actual values of pertinent outcomes that were not included during the calibration was evaluated [21, 28]. As shown in Figure 13, the results remained largely unaffected when several kinetic and stoichiometry parameters were modified. However, a slight difference was noted between the calibration and validation results due to the moderate level of contaminants observed during the year. After modifying additional sensitivity parameters, the validation and calibration operations yielded findings that fell within the specified RMSE and R limits (Table 6).

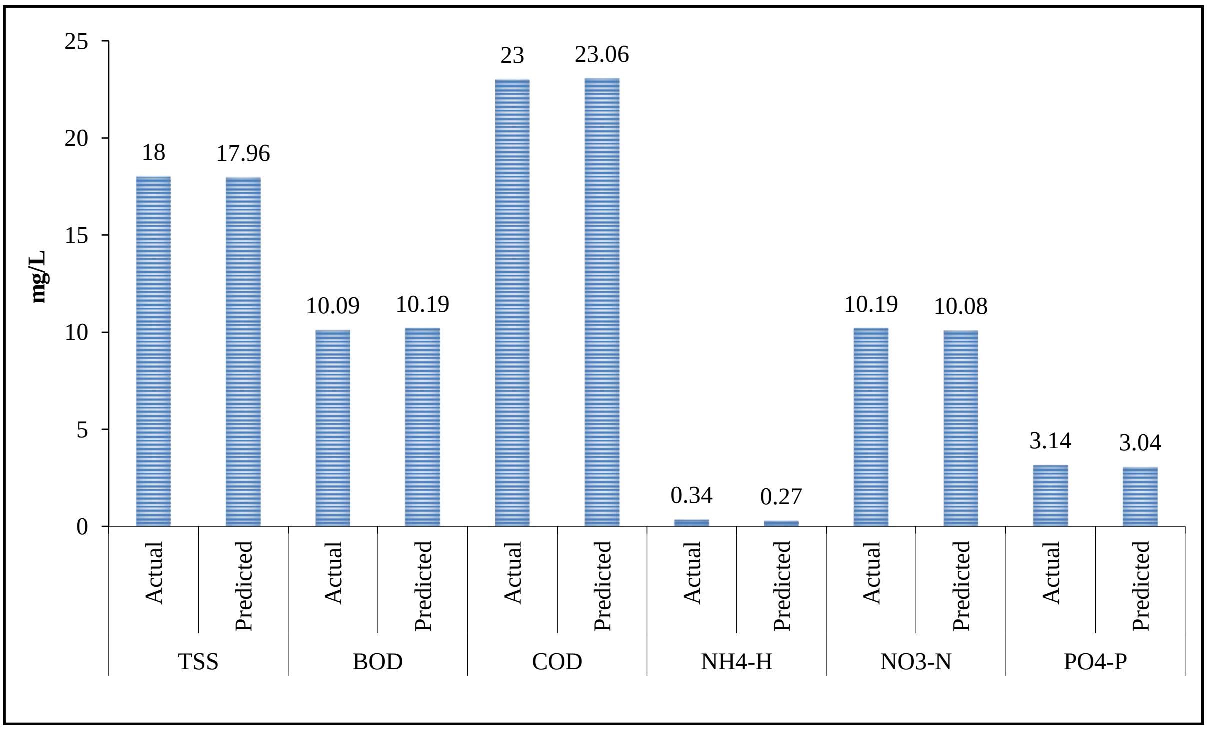

Figure 13. Validation of the actual and predicted values

Table 6. R and RMSE values were modified for calibration and verifications

Parameter	R-value for Autumn and winter averages	RMSE value for autumn and winter averages	R-value for spring and summer averages	RMSE value for spring and summer averages
TSS	0.88	0.0002	0.87	0.0001
BOD	0.86	0.0013	0.86	0.0006
COD	0.87	0.0003	0.89	0.0002
$NH4^+$-N	0.89	0.009	0.88	0.06
NO_2^--N	0.89	0.014	0.87	0.011
NO_3^--N	0.91	0.0019	0.89	0.0006
PO4-P	0.82	0.002	0.87	0.011

3.4. Sensitivity Analysis

Sensitivity analysis provides indicators of those variables that influence the operations to ensure optimal performance. Given that sensitivity analysis employs simulation rather than actual tests in treatment in the treatment plants, it also saves time [29]. SVI has been widely applied in previous research to assess the impact of biological variables or physical or chemical processes on sludge characteristics. In this study, SVI was applied to ascertain the required rate of sludge recycling or to compute the possible concentration of MLSS in the aeration tank. SVI was primarily employed to monitor the performance of wastewater treatment plants and assess the settling properties of various sludges. The final sludge volume was determined by the initial settling rate and the sludge behavior as it became more concentrated. If the SVI is an essential indicator of the solids that make up AS, then one would anticipate a systematic correlation between the concentration of sludge solids and SVI.

Figure 14 shows the effect of SVI on the effluents of A-STP. When the SVI is 50 ml/g, the values of COD, BOD, TSS, PO4-P, NH4, and NO3 are 32, 12, 30, 2, 0.2, and 14 mg/L, respectively. However, as SVI increased and reached 350 ml/g, a system failure was encountered, and the pollutants COD, BOD, and TSS departed from the required parameters with values of 102, 50, and 100 mg/L, respectively. Nitrates, phosphates, and ammonia were not affected by the precipitation processes, as they mainly took the form of ions. Only those pollutants with precipitable properties (particular material) were affected in the process. A lower SVI also corresponds to a better removal of COD, BOD, and TSS, which is consistent with the findings in the previous study [30, 31], where this study suggests that an increase in SVI leads to an increase in filamentous bacteria growth, which in turn causes system deterioration, a finding that aligns with the current study by Nile & Faris [31]. The degradation started at 250 ml/g, and the best SVI values in the extended aeration system ranged between 50 and 110. Therefore, the effluent concentrations matched the specifications.

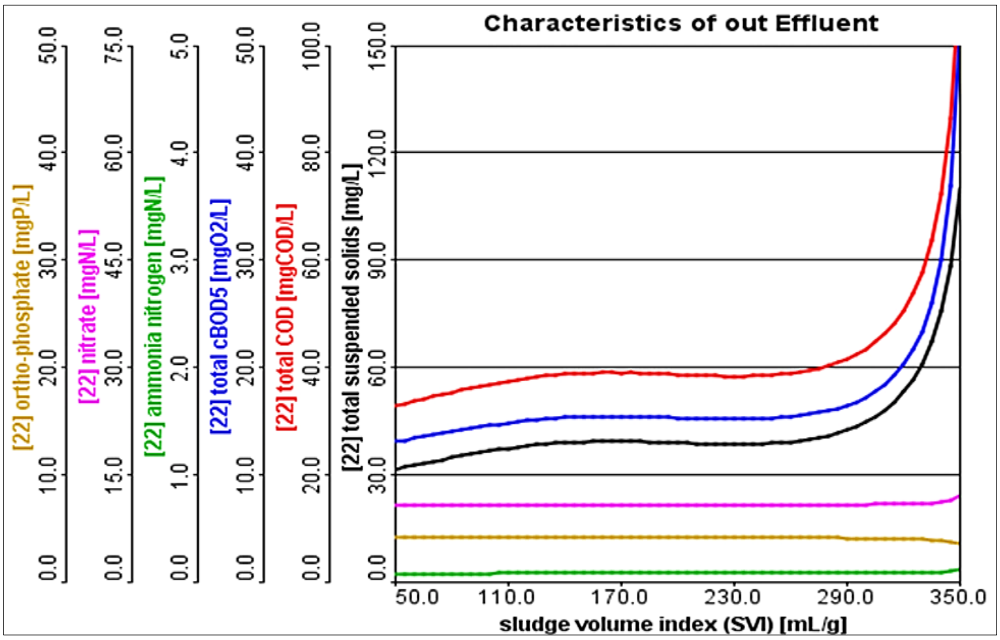

Figure 14. Sludge volume index

Stabilizing and removing pollutants from wastewater are one of most important biological processes in treatment plants. Given that these processes take place in SSBs, the design and operational study of these basins are two of the main tasks of treatment plants. Figure 15 presents a sensitivity analysis of the SSB in the A-STP. This analysis examined the impact of expanding the SSB's surface area on the quality of waste removal from those fluids originating in the basin, including COD, BOD, TSS, PO4, NH3, and NO3. Results show that when the SSB area increased from 804 m^2 to 3216 m^2 (representing the entry area of all four basins), the percentages of pollutants in the basin's output decreased from 65, 18, 44, 2, 0.2, and 14 mg/L to 33, 9, 16, 2, 0.2, and 14 mg/L. The results demonstrate that when the sedimentation basin's area increases from 804 m^2 to 3216 m^2, representing the entry area of all four basins in treatment process, the percentages of pollutants in the basin's output drop from 65, 18, 44, 2, 0.2, and 14 to 33, 9, 16, 2, 0.2, and 14 mg/L, respectively. This means that the sedimentation tank works efficiently to remove the incoming pollutants and that it gets enough time to do so. Increasing the surface area led to good sedimentation processes due to the high HRT values. Where increasing HRT means giving sufficient time for MLSS to precipitate well. In confirmation of this, studies have indicated that the surface area increases the residence time and thus improves the deposition processes [32]. We also observed that the sedimentation processes did not affect the ions. Because they are dissolved substances, the ions do not precipitate.

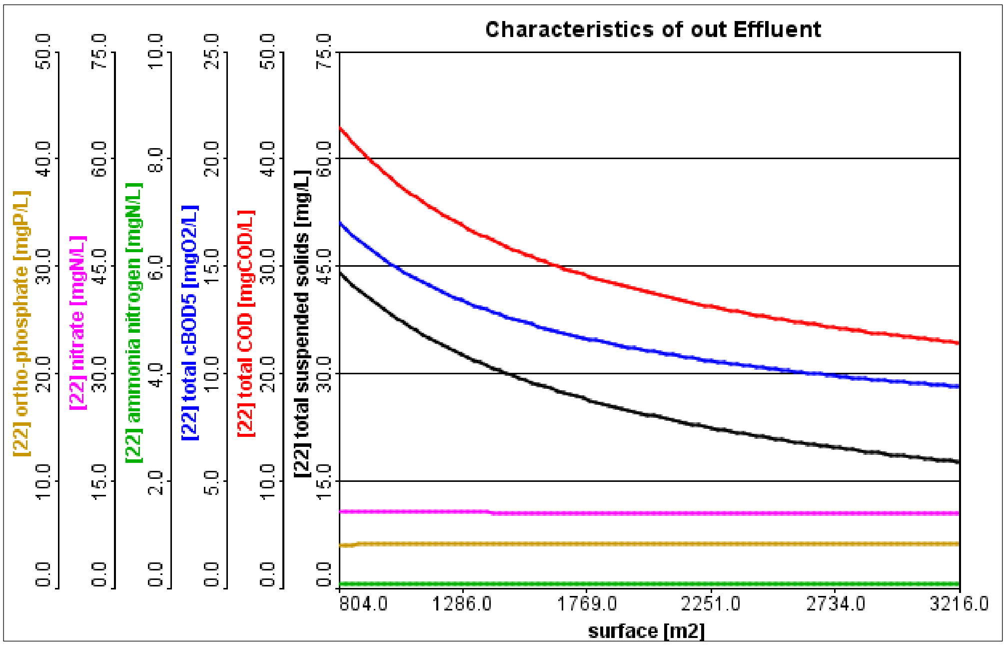

Figure 15. Surface area of sedimentation tank

The extended treatment plants for wastewater produce a small amount of waste solids because the SRT exceeds 24 days. Figure 16 shows the effect of the WAS from the SSB on the effluents COD, BOD, TSS, PO4-P, NH4, and NO3. As the discharge of excess sludge increased from 250 m^3/d to 4500 m^3/d, the values of COD, BOD, TSS, PO4-P, NH4, and NO3 changed from 22, 6, 21, 2.2, 0.2, and 9 mg/L to 26, 13, 14, 2, 0.2, and 12 mg/L, respectively. The increased flow of excess sludge also increased the reduction of TSS concentrations, but the BOD concentrations increased in the outlet due to the reduction of MLSS concentrations, which represent the concentrations of microorganisms in the aeration basin where an excessive removal of large amounts of MLSS from the system will reduce TSS concentrations and increase BOD concentrations. This result is consistent with the findings reported by Alattabi et al. [33]. Previous studies have also noted that reducing the processing of organic materials enhances SRT, lengthens its oxidation time, and triggers endogenous respiration. However, internal respiration increases cell debris and TSS concentrations.

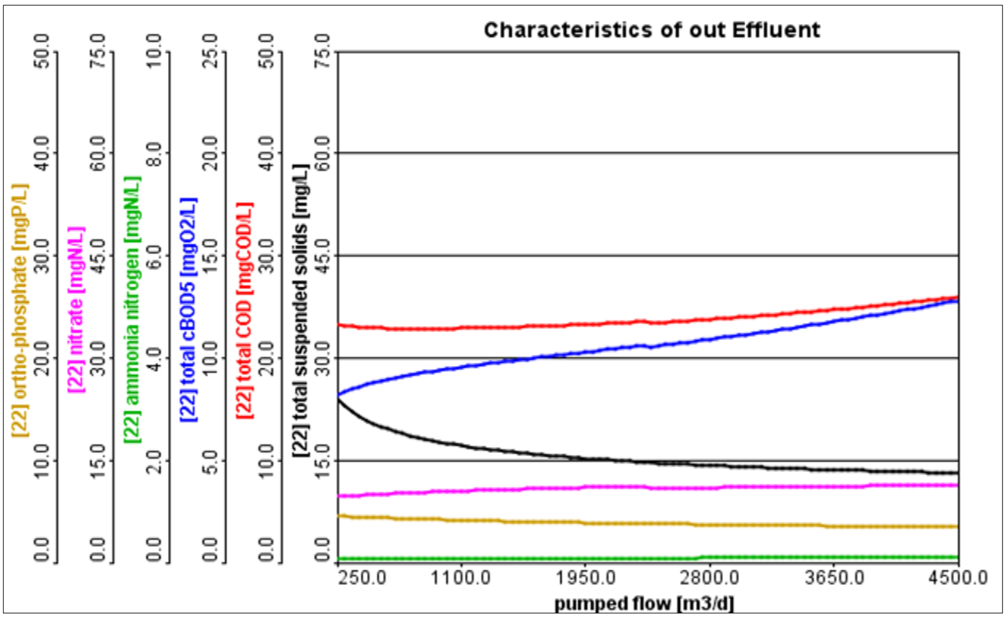

Figure 16. Pumped flow

The maximum SV of solids is an important parameter in clarifier operation and design. The acquired SVs were used in this study to generate a mass flow curve that guides the calculation of the settling basin area necessary for the thickening function. SV was used to determine the appropriate dimensions of the clarification basin. The accuracy of sedimentation velocities collected from repeated sedimentation tests will impact the performance of the SSBs [34]. Figure 17 shows the effect of the maximum SV of the SSBs on the effluents COD, BOD, TSS, PO4-P, NH4, and NO3. Increasing the maximum SV from 50 m/d to 500 m/d would reduce the indicated concentrations from 67, 18, 46, 3, 0.2, and 16 mg/L to 33, 9, 16, 3, 0.2, and 16 mg/L, respectively. Meanwhile, at a maximum SV of 230 m/d, the sedimentation process stabilized and thus no longer need to be increased further. Previous studies indicate that the maximum SV depends on several factors, the most important of which are the size of the sedimentable particles and the floc process. However, given that secondary sludge is less dense than primary sludge, therefore secondary sludge requires sufficient volume and surface area. Extended aeration weakens the floc process due to endogenous respiration.

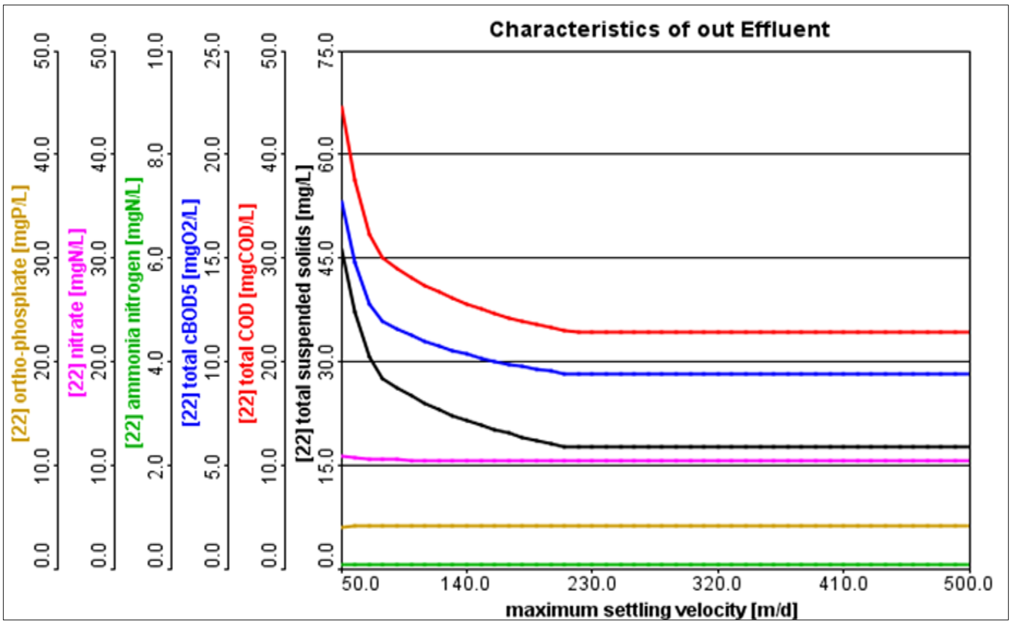

Figure 17. Maximum settling velocity

Sewage temperature is a significant parameter that affects biological treatment, aquatic organisms, and the suitability of water for various purposes [35]. The rise in sewage temperature may result in alterations in sewage, including a reduction in the dissolution of oxygen in water (reducing the saturation concentration Cs), acceleration of oxygen adsorption, rise in bacterial activity, and changes in the rate of gas transfer to and from the water, thus increasing the reaeration coefficient (K2) Furthermore, warm water exhibits lower solubility for oxygen compared with cold water. The saturation level of dissolved oxygen is influenced by changes in temperature [36, 37]. Hazen (1904) proposed that suspended molecules settle quicker when the liquid is warmer and added that the settling tank works twice as hard in summer as in winter [6]. Wells & LaLiberte (1998) proposed that when temperature variances are reported in settling tanks, particularly during winter, the impacts of temperature on the modeling of the settling tank should be considered [36].

Kriš & Hadi (2008) discovered that a reduction in air temperature leads to an increase in excessive effluent TSS [9]. Figure 18 shows the effect of the liquid temperature of the SSBs on the effluents COD, BOD, TSS, PO4-P, NH4, and NO3. Increasing the liquid temperature from 18 °C to 37 °C reduced the values of COD, BOD, TSS, PO4-P, NH4, and NO3 from 60, 35, 21, 2, 4.17, and 18.16 mg/L to 13.6, 3.55, 16.7, 3, and 7.15 mg/L, respectively, thereby confirming that liquid temperature affects all types of pollutants. The concentrations of COD and BOD decreased in response to increasing temperature in order to enhance the effectiveness of the metabolic processes carried out by microorganisms, thus promoting the decomposition of organic materials and reducing their concentrations. This finding demonstrates the acceleration of oxygen absorption, a decrease in its quantity in the SSBs, and an increase in plankton sedimentation. In the sludge liner of the clarification basin, the cost of a drop in the amount of TSS in the clarified effluent shows the efficiency of the treatment process for the settling basin. Additionally, as the liquid temperature increases, the viscosity increases, thus enhancing the flocculation process and forming large blocks that settle at the bottom of the SSB.

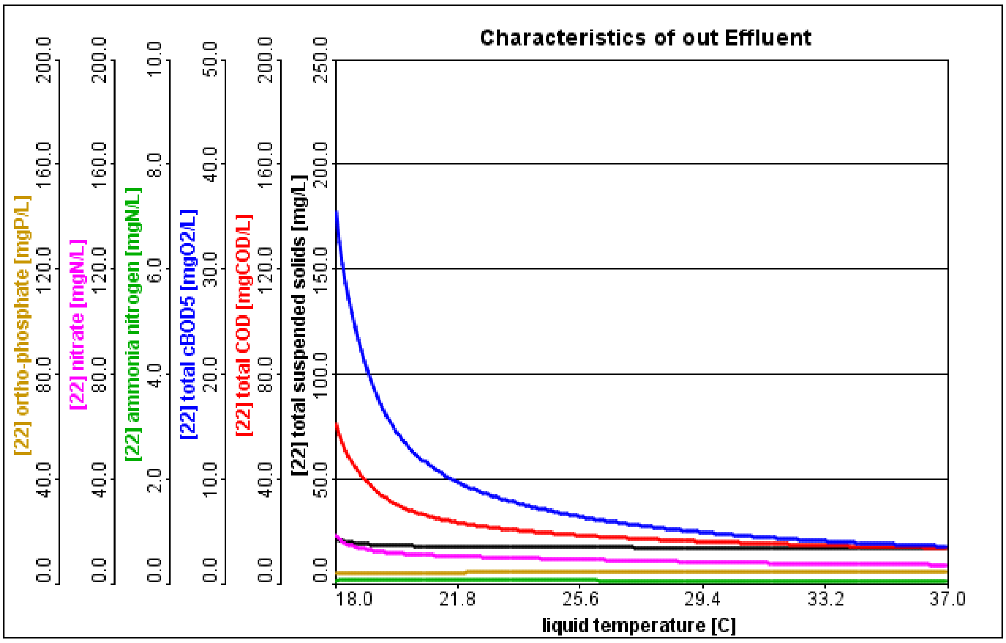

Figure 18. Liquid Temperature

4. Conclusion

Stabilizing pollutants is one of the processes of the Al-Hur sewage treatment unit (A-STP), which is characterized by the final clarification basins. For the first time, this study employed the GPS-X model to investigate and assess the sensitivity of a full-scale sedimentation basin. We regard the GPS-X model as an easy and simple tool for testing the behavior and sensitivity of the secondary sedimentation basin. We evaluated the secondary sedimentation basin's performance based on three factors: one practical factor (effluent pollutants) and two model parameters (state point analysis and sludge concentration in layers). The study led to the following conclusions: The state point analysis indicated that the best concentration of MLSS was 3000 mg/L. According to the study, the last three layers at the bottom of the sedimentation basin have a sludge concentration of 7000 mg/L. Increasing the sludge Sludge Volume Index (SVI) resulted in a decrease in the removal of pollutants such as COD, BOD, PO4, NH3, and NO3. This, in turn, caused the A-STP to deviate from the required parameters, making the secondary sedimentation basin less efficient. The greater the surface area of the secondary sedimentation basin, the better its efficiency. The increase in WAS was positive on TSS and negative on BOD. The increase in the underflow rate (RAS) resulted in a rise in the concentration of pollutants (COD, BOD, PO4, NH3, and NO3) in the MLLS of the return-activated sludge to the aeration basin, thereby enhancing the plant's treatment efficacy. The concentration of pollutants (COD, BOD, PO4, NH3, and NO3) in effluent waste went down when the maximum settling speed went up. This made treatment work better and made the sedimentation basin even more efficient. The increase in liquid temperature led to a decrease in the concentration of pollutants in effluent waste, which increased treatment efficacy. The physical properties of the secondary sedimentation basin, except for temperature, did not affect the ions (NO3, PO4, and NH4).

5. Declarations

5.1. Author Contributions

Conceptualization, B.K.N. and A.M.F.; methodology, S.A.H.; validation, B.K.N., A.M.F., and S.A.H.; formal analysis, B.K.N., A.M.F., and S.A.H.; investigation, B.K.N., A.M.F., and S.A.H.; writing—original draft preparation, B.K.N., A.M.F., and S.A.H.; writing—review and editing, B.K.N., A.M.F., and S.A.H. All authors have read and agreed to the published version of the manuscript.

5.2. Data Availability Statement

The data presented in this study are available in the article.

5.3. Funding

The authors received no financial support for the research, authorship, and/or publication of this article.

5.4. Acknowledgements

The authors would like to thank the Al-Hur sewage treatment plant (A-STP) for their collaboration during this work. Also, we would like to thank the directory of sewage treatment of Kerbala Government. The authors thanking Dr. Mohammad Abd AlRazaq for his assistant during the work.

5.5. Conflicts of Interest

The authors declare no conflict of interest.

6. References

[1] Patziger, M., Kainz, H., Hunze, M., & Józsa, J. (2012). Influence of secondary settling tank performance on suspended solids mass balance in activated sludge systems. Water Research, 46(7), 2415–2424. doi:10.1016/j.watres.2012.02.007.

[2] Li, B., & Stenstrom, M. K. (2013). Research advances and challenges in one-dimensional mathematical modeling of secondary settling tanks—a critical review. 86th Annual Water Environment Federation Technical Exhibition and Conference, WEFTEC 2013, 6, 3934–3952. doi:10.2175/193864713813685458.

[3] Li, B. (2016). One-Dimensional Modeling of Secondary Settling Tanks. The Regents of the University of California, California, United States.

[4] Mashi, A. L., & Rahama, M. S. (2015). Effects of Sludge Settleability in Final Sedimentation Tank. International Journal of Scientific & Engineering Research, 6(7), 2229–5518.

[5] Ekama, G. A., & Marais, P. (2004). Assessing the applicability of the 1D flux theory to full-scale secondary settling tank design with a 2D hydrodynamic model. Water Research, 38(3), 495–506. doi:10.1016/j.watres.2003.10.026.

[6] Hazen, A. (1904). On sedimentation. Transactions of the American Society of Civil Engineers, 53(2), 45-71. doi:10.1061/TACEAT.0001655.

[7] Dick, R. I., & Vesilind, P. A. (1969). The Sludge Volume Index: What Is It? In Journal (Water Pollution Control Federation), 41(7), 1285–1291.

[8] Mursalim, I. A., Pallu, M. S., Selintung, M., & Rahim, I. R. (2021). The effectiveness of increasing the amount of Return Activated Sludge (RAS) in wastewater with a combination biofilter system on bulking parameters. IOP Conference Series: Earth and Environmental Science, 841(1), 12026. doi:10.1088/1755-1315/841/1/012026.

[9] Kriš, J., & Hadi, G. A. (2008). Study the effect of temperature on sedimentation tanks performance. Water Supply and Water Quality. 8th International Scientific and Technical Conference on Water Supply and Water Quality, 439–453.

[10] Raeesh, M., Devi, T. T., & Hirom, K. (2023). Recent Developments on Application of Different Turbulence and Multiphase Models in Sedimentation Tank Modeling—a Review. Water, Air, and Soil Pollution, 234(1), 5. doi:10.1007/s11270-022-06007-8.

[11] Lasaki, B. A., Maurer, P., & Schönberger, H. (2023). Effect of coupling primary sedimentation tank (PST) and microscreen (MS) to remove particulate organic carbon (POC): a study to mitigate energy demand in municipal wastewater treatment plants. Sustainable Environment Research, 33(1), 25. doi:10.1186/s42834-023-00186-7.

[12] Dairi, S., Khoualdia, W., Mrad, D., Bouamrane, A., Djebbar, Y., & Abida, H. (2023). Improving secondary settling tanks performance by applying CFD models for design and operation. Water Supply, 23(6), 2313–2331. doi:10.2166/ws.2023.136.

[13] Wu, X., Wei, J., Shen, L., & Li, X. (2024). Investigation of the Influence of Operating Parameters on the Settling Performance of a Vertical Sedimentation Tank Through Computational Fluid Dynamics Simulations. Water, Air, and Soil Pollution, 235(5), 1–14. doi:10.1007/s11270-024-07110-8.

[14] Poorkarimi, A., Mafakheri, K., & Maleki, S. (2024). Effect of inlet and baffle position on the removal efficiency of sedimentation tank using Flow-3D software. Journal of Hydraulic Structures, 9(4), 76–87.

[15] Hydromantis, E. S. S. (2017). Inc. GPS-X Technical Reference; Hydromantis ESS. In Inc.: Hamilton, ON, Canada.

[16] Faris, A. M., Zwain, H. M., Hosseinzadeh, M., & Siadatmousavi, S. M. (2022). Modeling of novel processes for eliminating sidestreams impacts on full-scale sewage treatment plant using GPS-X7. Scientific Reports, 12(1), 2986. doi:10.1038/s41598-022-07071-0.

[17] Jasim, N. A. (2020). The design for wastewater treatment plant (WWTP) with GPS X modelling. Cogent Engineering, 7(1), 1723782. doi:10.1080/23311916.2020.1723782.

[18] Mannina, G., Cosenza, A., Vanrolleghem, P. A., & Viviani, G. (2011). A practical protocol for calibration of nutrient removal wastewater treatment models. Journal of Hydroinformatics, 13(4), 575–595. doi:10.2166/hydro.2011.041.

[19] Nile, B. K., Faris, A. M., Alesary, H. F., Jafar, N. N. A., Ismail, H. K., Abdulredha, M., Al Juboury, M. F., Hassan, W. H., Ahmed, L. M., Abid, H. R., & Barton, S. (2024). Simulation study of a practical approach to enhance cadmium removal via biological treatment by controlling the concentration of MLSS. Scientific Reports, 14(1), 1714. doi:10.1038/s41598-023-50843-5.

[20] Rice, E. W., Bridgewater, L., & American Public Health Association (Eds.). (2012). Standard methods for the examination of water and wastewater, Volume 10, American Public Health Association, Washington D.C., United States.

[21] Hamad, N. F., Nile, B. K., Alamir, H. T. A., Faris, A. M., Ismail, H. K., Hassan, W. H., Ahmed, L. M., Alesary, H. F., & Barton, S. (2023). Case study of hydrogen sulfide release in the sulfate-rich sewage drop structure. Journal of Water and Climate Change, 14(10), 3713–3725. doi:10.2166/wcc.2023.283.

[22] Al-Amery, Z. M., Alyaseri, I., & Al-Saadi, R. J. (2023). Deterioration of Wastewater Treatment Processes in Iraq: A Case Study from Al-Samawah. AIP Conference Proceedings, 2806(1), 0163663. doi:10.1063/5.0163663.

[23] Takács, I., Patry, G. G., & Nolasco, D. (1991). A dynamic model of the clarification-thickening process. Water Research, 25(10), 1263–1271.

[24] Faris, A. M., Zwain, H. M., Hosseinzadeh, M., Majdi, H. S., & Siadatmousavi, S. M. (2022). Start-up and operation of novel EN-MBBR system for sidestreams treatment and sensitivity analysis modeling using GPS-X simulation. Alexandria Engineering Journal, 61(12), 10805–10818. doi:10.1016/j.aej.2022.04.026.

[25] Hassan, W. H., Faris, A. M., & Faisal, A. A. H. (2024). Using TOXCHEM model for simulation the hydrogen sulfide behavior in a full-scale MBBR process. Desalination and Water Treatment, 317, 100244. doi:10.1016/j.dwt.2024.100244.

[26] Zwain, H. M., Nile, B. K., Faris, A. M., Vakili, M., & Dahlan, I. (2020). Modelling of hydrogen sulfide fate and emissions in extended aeration sewage treatment plant using TOXCHEM simulations. Scientific Reports, 10(1), 22209. doi:10.1038/s41598-020-79395-8.

[27] Zwain, H. M., Faris, A. M., Hassan, W. H., Soomro, S. e. hyde., & Majdi, A. (2024). Modeling the effects of sidestreams recycling on wastewater treatment plant performance operated by anaerobic-anoxic-oxic (A2/O) processes using GPS-X8 simulation. Results in Engineering, 22, 102173. doi:10.1016/j.rineng.2024.102173.

[28] Mu'azu, N. D., Alagha, O., & Anil, I. (2020). Systematic modeling of municipal wastewater activated sludge process and treatment plant capacity analysis using GPS-X. Sustainability (Switzerland), 12(19), 8182. doi:10.3390/su12198182.

[29] Faris, A. M., Nile, B. K., Mussa, Z. H., Alesary, H. F., Al Juboury, M. F., Hassan, W. H., Al-Bahrani, H. A., & Barton, S. (2022). Fate and emission of methyl mercaptan in a full-scale MBBR process by TOXCHEM simulation. Journal of Water and Climate Change, 13(6), 2386–2398. doi:10.2166/wcc.2022.438.

[30] Wang, J., Li, Q., Qi, R., Tandoi, V., & Yang, M. (2015). Sludge bulking impact on relevant bacterial populations in a full-scale municipal wastewater treatment plant. Process Biochemistry, 49(12), 2258–2265. doi:10.1016/j.procbio.2014.08.005.

[31] Nile, B. K., & Faris, A. M. (2018). The effect of MLSS values on removal of COD and phosphorus using control method of return activated sludge concentration. Journal of Engineering and Applied Sciences, 13(22), 9730–9734. doi:10.3923/jeasci.2018.9730.9734.

[32] Amanatidou, E., Samiotis, G., Trikoilidou, E., Pekridis, G., & Taousanidis, N. (2015). Evaluating sedimentation problems in activated sludge treatment plants operating at complete sludge retention time. Water Research, 69, 20–29. doi:10.1016/j.watres.2014.10.061.

[33] Alattabi, A. W., Harris, C. B., Alkhaddar, R. M., Ortoneda-Pedrola, M., & Alzeyadi, A. T. (2019). An investigation into the effect of MLSS on the effluent quality and sludge settleability in an aerobic-anoxic sequencing batch reactor (AASBR). Journal of Water Process Engineering, 30, 100479. doi:10.1016/j.jwpe.2017.08.017.

[34] Ong, S. L. (1992). Effect of measurement error of settling velocity on secondary sedimentation tank design. Water Environment Research, 64(2), 104–110. doi:10.2175/wer.64.2.2.

[35] Metcalf, & Eddy. (2022). Wastewater Engineering: Treatment and Resource Recovery. McGraw Hill Education, New York, United States.

[36] Wells, S. A., & LaLiberte, D. M. (1998). Winter temperature gradients in circular clarifiers. Water environment research, 70(7), 1274-1279. doi:10.2175/106143098X123642.

[37] Alisawi, H. A. O. (2020). Performance of wastewater treatment during variable temperature. Applied Water Science, 10(4), 89. doi:10.1007/s13201-020-1171-x.